Catalysis Science & Technology

ROYAL SOCIETY OF CHEMISTRY

PAPER

View Article Online
View Journal | View Issue

Check for updates

Cite this: *Catal. Sci. Technol.*, 2021, 11, 5472

Polymethylaluminoxane organic frameworks (sMAOF) – highly active supports for slurry phase ethylene polymerisation†

Alexander F. R. Kilpatrick, [a] Harry S. Geddes, [b] Zoë R. Turner, [a] Jean-Charles Buffet, [a] Andrew L. Goodwin *[b] and Dermot O'Hare *[a]

Received 29th April 2021,
Accepted 9th July 2021

DOI: 10.1039/d1cy00767j

rsc.li/catalysis

A series of modified solid polymethylaluminoxane (sMAO) catalyst supports have been developed for slurry phase ethylene polymerisation, using aryl di-ol modifier groups. Characterisation using ICP-MS analysis, X-ray total scattering, SEM–EDX, diffuse FT-IR and solid state NMR spectroscopy shows that the organic linker groups are uniformly distributed in a proposed organic framework stucture we call a "sMAOF". When used as a support for *rac*-ethylene{bis(1-indenyl)} zirconium dichloride, (EBI)$ZrCl_2$, these linker modified sMAOF materials provide a 40% enhancement in polymerisation activity with respect to unmodified sMAO: activities of 163 × 10^3 and 116 × 10^3 kg_{PE} mol_{Zr}^{-1} h^{-1} at 80 °C for (EBI)$ZrCl_2$ supported on sMAOF(1,4-HO(C_6F_4)OH) and sMAO, respectively. The observed activity increase is correlated with the higher BET surface area and increased porosity in the linker modified sMAOF activating support.

Introduction

Methylaluminoxane (MAO) is the most commonly used activator and co-catalyst for single-site metallocene and post-metallocene complexes in homogeneous olefin polymerisation.[1–3] There has been significant progress in the past decade in the characterisation of MAO and its function as a source of an electrophilic cation, $[AlMe_2]^+$, which plays a key role in the activation of metallocene complexes.[4–16] The importance of MAO has spurred recent interest in improving activators for olefin oligomerisation and (co)polymerisation catalyst systems, including soluble $[NR_4]^+[B(C_6F_5)_4]^-$ co-catalysts containing long *N*-alkyl chains,[17,18] weakly coordinating anions based on alkoxyaluminates,[19] chlorinated carborane ammonium salts,[20] a dinuclear aluminium cationic cluster,[21] and a neutral fluoroarylborane.[22]

A well-known chemical treatment of MAO utilises hindered phenols such as 2,6-di-*tert*-butyl-4-methylphenol (BHT) to scavenge the "free" trimethylaluminium (TMA) present in MAO solutions,[23–28] yielding a hindered phenoxide-alkylaluminium species $MeAl(bht)_2$ (bht = BHT phenolate) that does not interact with the catalyst complex. Zaccaria *et al.* proposed that BHT in excess converts some of the remaining "structural" TMA in MAO into analogous "structural" $AlMe_2(bht)$ molecules in a modified aluminoxane (MMAO) cluster.[29,30] This TMA-depleted MMAO is also an effective catalyst activator which can increase the activity and molecular weight of the resulting polymer,[31–33] depending on the nature of the pre-catalyst complex.[34]

Extensive computational studies of MAO[35–44] indicate that with increasing aggregation of [Al(O)Me] units the structure changes from sheets to nanotubes to cages,[45,46] which reach the size domain of MAO (typically 1000–3000 g mol^{-1}).[47]

Linnolahti and co-workers have proposed that the cage $(AlOMe)_{16}(AlMe_3)_6$ represents the most stable model MAO cluster,[40,47] which is supported by several other combined theoretical and experimental studies.[4,7,11–14,16,29,48] This cage features "structural" TMA molecules binding in three different cluster environments (Chart 1), that behave quite differently.[10] Site III (with two bridging methyl groups) is more prone to release $[AlMe_2]^+$ and $AlMe_3$, and therefore

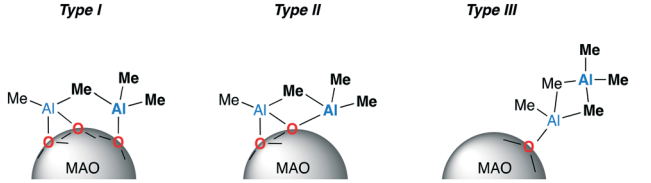

Chart 1 "Structural" $AlMe_3$ molecules (in bold), binding different Al-sites: one type I, one type II and two type III of the DFT optimised MAO model cluster proposed by Linnolahti and co-workers.[40,47]

[a] *Chemistry Research Laboratory, Department of Chemistry, University of Oxford, 12 Mansfield Road, Oxford, OX1 3TA, UK. E-mail: Dermot.ohare@chem.ox.ac.uk*
[b] *Inorganic Chemistry Laboratory, University of Oxford, South Parks Road, Oxford, OX1 3QR, UK. E-mail: Andrew.goodwin@chem.ox.ac.uk*

† Electronic supplementary information (ESI) available: Experimental details (general procedures, syntheses and ethylene polymerisation), additional characterising data (solution and solid state NMR spectroscopy, DRIFTS, X-ray PDF, BET surface area), SEM images for sMAOF and polyethylene samples. See DOI: 10.1039/d1cy00767j

likely responsible for the abstracting capability of MAO.[10] Furthermore, upon reaction with Brønsted acids like BHT, the "structural" TMA molecules bound at type III sites are largely released,[30] followed by structural rearrangements that "annihilate" these type III sites.[28] Type I and type II sites (with one bridging Me and a proximal two-coordinate O atom) are predicted to bind "structural" $AlMe_2$(bht) rather strongly, and are therefore assigned to "structural" $AlMe_2$(bht) that is not released by the cages.[28]

In slurry phase polymerisation, the combination of MAO, an inert inorganic carrier material (usually silica) and a precatalyst complex has been dubbed the "Holy Trinity" of supported single-site catalysts.[49] In recent years, carrier-free systems have been developed featuring an activating support material,[50] which can be combined with the precatalyst complex in a single synthetic step.[51–55] In principle, these 'self-supported' systems provide a cost-effective way of designing solid catalysts for olefin polymerisation to produce industrial-grade polyolefins.[56–58]

Upon immobilisation, the molecular precursor complex undergoes reaction with the activator surface while maintaining most of the ligand sphere of the parent molecule.[59] Therefore, research into optimising single-site catalyst performance has focussed mainly on varying the structure of the precatalyst complex *via* the active metal centre and its ancillary ligands.[60,61] However, modifying the structure of the activating support itself can have a significant effect on the polymerisation activity and allows for fine-tuning of polymer properties, such as molecular weights, and particle morphology.[62–65] In the case of heterogenised-MAO catalyst systems the support can, for example, influence the concentration of "free" TMA,[66,67] but it is assumed that the structure and chemical environment of the active polymerising species are not directly affected.[68]

Solid polymethylaluminoxane (sMAO) is an insoluble form of oligomeric MAO first disclosed in the patent literature, synthesised by reaction of benzoic acid with $AlMe_3$.[69] Particulate sMAO has an extremely low solubility in hydrocarbons (0.1 mol% in hexane at 25 °C, 0.4 mol% in toluene at 25 °C) and this significantly supresses reactor fouling when employed in polymerisation, yielding a polymer of uniform particle diameter. In 2015, O'Hare and co-workers reported the laboratory scale synthesis and detailed characterisation of sMAO,[70] and demonstrated its function as a solid-phase support, scavenger and activator in slurry phase ethylene polymerisation.[71–73] Observed activities are remarkably higher for sMAO-based supported metallocene catalysts than for those based on MAO-impregnated inorganic supports; for example, sMAO-*rac*-ethylenebis(1-permethylindenyl) zirconium dichloride is over 3× more active than the analogous silica-supported MAO system (10.7×10^3 *vs.* 3.3×10^3 kg_{PE} mol_{Zr}^{-1} h^{-1} respectively).[74,75] Lamb *et al.* reported the treatment of sMAO with tris(pentafluorophenyl)borane and pentafluorophenol produces highly active modified-sMAO supports that show enhanced polymerisation activity with both *rac*-ethylenebis(1-indenyl) zirconium dichloride, (EBI)$ZrCl_2$,[76] and a range of unsymmetrical *ansa*-bridged permethylindenyl complexes.[77] It was postulated that the surface-bound C_6F_5 or C_6F_5O groups on the support lead to an increase in separation between the charged species formed after precatalyst activation, which in turn enhances the performance of the catalytically active species.[76] Very recently, Kilpatrick *et al.* reported an in-depth characterisation of the final functional catalyst in sMAO–zirconocene systems using high field solid state nuclear magnetic resonance (SSNMR) spectroscopy, SEM-EDX elemental mapping and diffuse-reflectance FT-IR spectroscopy.[78] These studies provided evidence for a secondary interaction between the proposed $[Cp'_2ZrMe]^+$ surface-bound species and the sMAO surface, which can influence catalytic activity. To extend these studies we targeted bifunctional modifiers with the aim of varying both the chemical and physical properties of the modified-sMAO activating support.

Silica-based catalyst supports bearing bifunctional organic groups such as hydroquinone were studied by Popoff *et al.*[79–81] $Zr(CH_2Ph)_4$ grafted onto a hybrid material with phenol grafting sites, $[(\equiv SiO)_2(AlOC_6H_4OH)(Et_2O)]$, afforded a monopodal tribenzyl surface species that was activated with $B(C_6F_5)_3$ to generate a cationic species with a di-ol spacer $[(\equiv SiO)_2(AlOC_6H_4–OZr(CH_2Ph)_2)(Et_2O)]^+[(PhCH_2)B(C_6F_5)_3]^-$ (Chart 2a).[81] This catalyst was tested for ethylene polymerisation capability, and showed a fourfold increase in productivity compared to that of the silica counterpart $[\equiv SiOZr(CH_2Ph)_2]^+[(PhCH_2)B(C_6F_5)_3]^-$, which was attributed to reduced surface interactions and increased electrophilicity. The related support materials $[(\equiv SiO)_2(AlO–C_6X_4–OH)(Et_2O)]$, where X = H or F, were used to tether the organometallic tungstenocarbyne complex $[W(\equiv C^tBu)(CH_2{}^tBu)_3]$ to yield the surface species $[(\equiv SiO)_2(AlO–C_6X_4–O–W(\equiv C^tBu)(CH_2{}^tBu)_2(Et_2O)]$ with X = H or F (Chart 2b).[79] Both H- and F-species were studied as catalysts for the self-metathesis reaction of propene to ethylene and 2-butenes, and reported activity values were two and three times higher, respectively, than the activity of the corresponding tungstenocarbyne complex directly grafted onto silica.

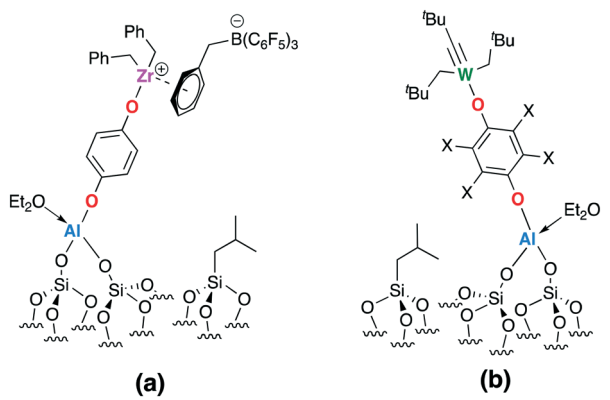

Chart 2 Hydroquinone-modified silica support materials reported by Popoff *et al.* with an immobilised (a) cationic zirconium complex and (b) tungsten alkylidene complex.[79,81]

Bifunctional additives have also been used to modify solution MAO, such as diols,[51] bisphenol A,[79] carbonates,[82] and boroxines.[83] Soga and co-workers reported the reaction of MAO with a small quantity of *p*-hydroquinone to obtain a modified solid MAO insoluble in toluene.[52] Ethylene and propylene homo- and copolymerisation were conducted with (EBI)$ZrCl_2$ and Cp_2ZrCl_2 using the modified MAO as co-catalyst both in the presence and absence of triisobutylaluminium. It was found that the modified MAO alone could not activate the (EBI)$ZrCl_2$ zirconocene catalyst, whereas polymers with high molecular weights were obtained when combined with triisobutylaluminium. The catalytic activity was markedly dependent on the mole ratio of *p*-hydroquinone to MAO as well as the amount of triisobutylaluminium.

Here, we describe the post-synthesis modification of sMAO using bi-functional organic compounds, in particular aromatic di-ols, with the objective of increasing the surface area of the material and hence improving its properties as a support for zirconocene precatalysts. We are also interested whether the use of these bifunctional additives will link together modified sMAO clusters to create new highly porous supports.

Results and discussion

Synthesis and characterisation of solid polymethylaluminoxane organic frameworks (sMAOF) with tetrafluorohydroquinone

Pentafluorophenol has shown a large boosting effect on the ethylene polymerisation activity of modified sMAO supports,[76,77] which can be attributed to the electron-withdrawing effect of this perfluoroaryl modifier, and its relative acidity (pK_a = 5.5 in water)[84] which ensures complete reaction with "structural" TMA present in sMAO. By analogy with BHT modified MAO solutions studied by the groups of Busico, Ehm and others,[23,24,26–30] we postulate that the modifier forms "structural" $(C_6F_5O)AlMe_2$ species bound to type I and/or type II sites on the modified sMAO clusters (Scheme 1).

Molecular methylaluminium aryloxide compounds are known with both bridging and terminal aryloxide ligands.[85–91] In the case of pentafluorophenol modified sMAO we postulate the OC_6F_5 group bridges two neighbouring Al centres, since the oxygen lone pair renders it a better bridging ligand than a Me ligand. NMR spectroscopy in THF-d_8 suggests that pentafluorophenol modified type I and type II sites release "free" $(C_6F_5O)AlMe_2$ species (detected as $(C_6F_5O)AlMe_2$·THF), but do not undergo significant ionisation. The ability of MAO to generate large anions with a delocalised negative charge has been proposed as one of the origins of the excellent co-catalytic properties of this aluminoxane.[92–95] Hence, we hypothesise that $(C_6F_5O)AlMe_2$ species bound to type I and/or type II sites will be more Lewis acidic and therefore likely have enhanced abstraction capabilities with zirconocene complexes.

As an entry point to the current study, tetrafluorohydroquinone and tetrafluoroterephthalic acid,

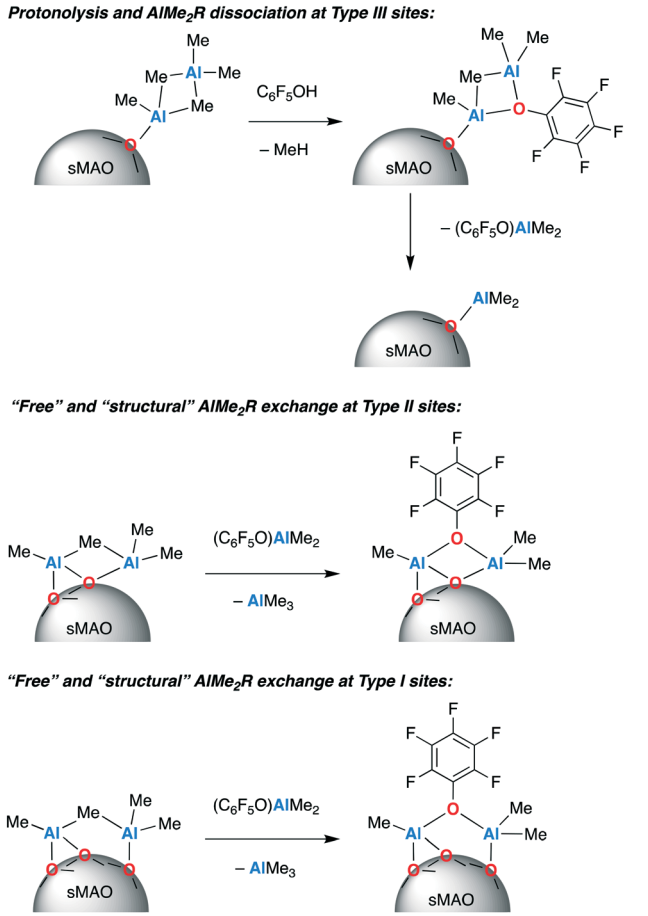

Scheme 1 Schematic to represent the proposed reaction of sMAO with C_6F_5OH modifier.

1,4-X(C_6F_4)X for X = OH (**A**) and COOH (**B**) were selected to study the linking effect of a different functional group (hydroxyl *vs.* carboxylic acid). The fluoride substituent on the aryl-linker for these groups provide a convenient handle for $^{19}F\{^1H\}$ NMR spectroscopy studies, and a possible electron withdrawing effect for the activating support.

The post-modification procedure was carried out according to published literature,[76] using initial modifier: aluminium ($[M]_0/[Al_{sMAO}]_0$) loadings of 0.025 and 0.05. In a typical experiment, commercially supplied sMAO[69] was suspended in toluene, to which a toluene solution of the modifier 1,4-HO(C_6F_4)OH (**A**) was slowly added. In the case of the modifier 1,4-HOOC(C_6F_4)COOH (**B**) which showed poor toluene solubility, the two solid reagents were combined in the same flask, to which toluene was added. The mixture was sonicated for 1 h, during which time the temperature increased from 25 to 45 °C. Upon addition of modifier **A** to sMAO, effervescence was observed, confirming a protonolysis reaction with concomitant release of methane gas. In the case of compound **B**, no reaction was observed. A control experiment was also carried out, using an identical procedure but without the addition of a modifying compound. After cooling to room temperature, the resultant slurry was then

treated with hexane to extract by-products and encourage precipitation of a colourless solid. After settling, the supernatant solution was removed and the solid samples were vacuum dried and isolated in good yield (56–81%). For brevity, each linker-modified solid polymethylaluminoxane framework prepared herein will be represented as sMAOF(x, M), where x is the $[M]_0/[Al_{sMAO}]_0$ loading in reactants, and M is the linker modifier compound.

The diffuse reflectance infrared Fourier transform (DRIFT) spectrum of sMAOF(0.05,**A**) was measured and compared to that of un-modified sMAO (Fig. S1†). The linker modified sample displayed a new IR band at 1652 cm^{-1} assigned to the aromatic ring stretching modes $\nu(C_{sp2}{=}C_{sp2})$ of the bridging $-O(C_6F_4)O-$ group.[96,97] No additional bands were observed in the hydroxyl region of the DRIFT spectrum (3550–3200 cm^{-1}) suggesting both of the O–H functionalities of the linker molecule have been deprotonated.

The linker modified sMAOF(**A**) samples were sparingly soluble in THF-d_8, allowing for their characterisation by solution NMR spectroscopy. The ^{1}H NMR spectrum of sMAOF(0.025,**A**) (Fig. S2†) shows the anticipated resonance between δ_H 0.03 and −1.57 ppm, assigned to the MAO backbone methyl groups, which is very broad due to the oligomeric nature of the material.[70] Within this broad feature are sharp signals at δ_H −0.60 and −0.96 ppm, assigned to $[AlMe_2(THF)_2]^+$ and $AlMe_3(THF)$ respectively, formed *via* THF association to ionised $[AlMe_2]^+$ and "free" TMA released on dissolution, respectively.[4]

The ^{1}H NMR spectrum of sMAOF(0.05,**A**) (Fig. S4†) does not show a sharp signal at δ_H −0.60 ppm, suggesting a lower extent of $[AlMe_2(THF)_2]^+$ ionisation for the sample with a higher linker modifier loading. The $^{19}F\{^1H\}$ NMR spectra of sMAOF(0.025,**A**) and sMAOF(0.05,**A**) (Fig. S3 and S5,† respectively) both show a single resonance at δ_F −167.6 ppm consistent with a $-O(C_6F_4)O-$ fragment which is symmetrically bound between two aluminoxane clusters. Theoretical calculations by Zaccaria *et al.* suggest that "structural" TMA molecules most strongly bound to type III site in MAO, and modified "structural" $AlMe_2R$ species are strongly bound to type I and II sites.[28] We therefore propose an analogous situation for sMAOF(**A**), with either a type I or type II site bearing the linker group (Chart 3). The $-O(C_6F_4)O-$ modified "structural" sites bound at both ends by aluminium are not expected to undergo significant ionisation. It is postulated that $[AlMe_2]^+$ and "free" TMA are released from type III sites carrying a "structural" TMA molecule.[10] However, the complexity of heterogeneous systems means that straightforward connections with the structure and reactivity of unmodified MAO in solution must be treated with caution,[67,68] hence these structures are tentatively proposed.

Solid state NMR spectroscopy (SSNMR) allows for further characterisation of poorly soluble samples (Fig. S6–S11†). Fig. 1 shows the $^{19}F\{^1H\}$ HP-DEC[98] spectrum of sMAOF(0.05, **A**), with a broad resonance at isotropic chemical shift δ_F −162 ppm confirming incorporation of the fluorinated aryl group in the sMAOF structure.

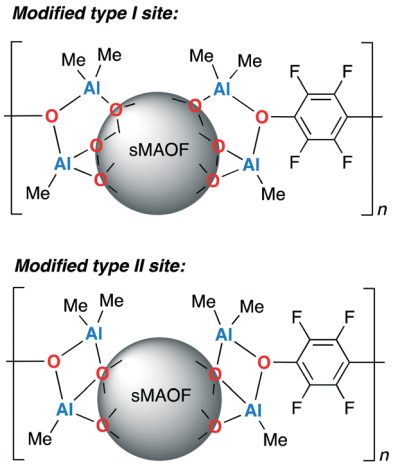

Chart 3 Simplified representation of the proposed sMAOF(A) structure.

Previous ^{13}C–^1H cross-polarisation magic angle spinning (CP-MAS) SSNMR studies of sMAO, synthesised from $AlMe_3$ and α-^{13}C labelled benzoic acid, revealed the presence of residual benzoate groups in the structure.[70]

The ^{13}C–^1H CP-MAS SSNMR spectrum of sMAOF(0.05,**A**) (Fig. 2) shows a backbone methyl resonance at δ_C −8.7 ppm and several overlapping resonances between δ_C 140–125 ppm, assigned to the aryl ^{13}C nuclei of the benzoate residues and the $-O(C_6F_4)O-$ linker groups in the proposed structure. The cross polarisation nucleus in the ^{13}C CP-MAS experiment was changed from ^1H to ^{19}F, which selectively transfers its polarisation to ^{13}C atoms in close proximity to the ^{19}F nucleus. The ^{13}C–$\{^{19}F\}$ CP-MAS SSNMR spectrum of sMAOF(0.05,**A**) (Fig. 2, inset) shows two resonances at δ_C 132.9 and 120.0 ppm, which are assigned to the *ortho*- and *ipso*-carbon atoms of the 1,4-bis(olate) modifying group which symmetrically bridges aluminoxane units in the proposed structure.

The specific surface area of the sMAOF(x,**A**) samples was determined by analysis of N_2 gas physisorption using Brunauer–Emmett–Teller (BET) theory.[99] The adsorption isotherm obtained (Fig. S12–S14†) is a cross between a type

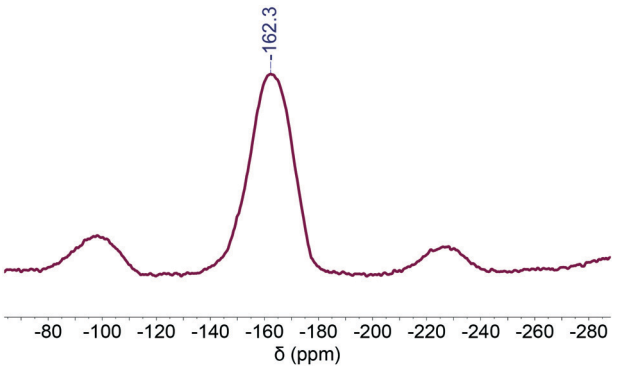

Fig. 1 $^{19}F\{^1H\}$ HP-DEC NMR spectrum of sMAOF(0.05,A) at 24 kHz spinning.

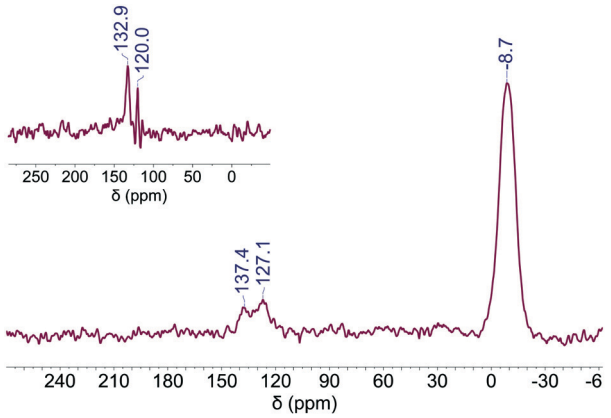

Fig. 2 ^{13}C–{^{1}H} and ^{13}C–{^{19}F} (inset) CP-MAS SSNMR spectra (10 kHz spinning) of sMAOF(0.05,**A**).

Ib and type II isotherm of the IUPAC classification,[100] which suggests pore size distributions over a broad range including wide micropores (of width <1 nm) and possibly narrow mesopores (<2.5 nm).

Interestingly, the BET surface area of sMAOF(**A**) samples are significantly higher than the control (688.9 $m^2\ g^{-1}$), and there is a general increase in surface area with increasing modifier loading (750.6–895.7 $m^2\ g^{-1}$).

The *t*-plot analysis[101,102] reveals a progressive increase in micropore area and micropore volume with increasing modifier loading (Table 1). This is accompanied by a general decrease in external surface area (= BET surface area – *t*-plot micropore area) with linker **A** modification, such that the ratio of micropore area/external surface area steadily increases, ranging from 0.49 in the control sMAO to 1.44 in sMAOF(0.05,**A**) (Tables S1–S4†). The observed increase in specific surface area and porosity is consistent with the proposed net exchange of Al-bound μ-methyl groups with the bifunctional linker groups, which creates 'channels' on the sMAO surface leading to the proposed framework structure.

Metal–organic framework (MOF) materials are gaining increasing attention as model catalysts and/or catalyst supports for polymerisation.[103,104] In 2015, Klet *et al.* reported the immobilisation of Zr-benzyl species on the node of a well-defined framework Hf-NU-1000, to afford active solid catalysts for olefin polymerisation.[105] Recently, Lin and co-workers described a Zr-benzene tricarboxylated MOF activated with MMAO which affords a robust catalyst system with a long lifetime, producing high M_w polyethylene.[106] In contrast to these highly crystalline MOF materials, the sMAOF activating support and catalysts described herein are amorphous.

A modifier loading study was carried out to determine which ratio of linker **A** would produce the best polymerisation activity, with analytical data summarised in Table 1. Samples of sMAOF(**A**) at higher linker loadings ($[M]_0/[Al_{sMAO}]_0$ = 0.10, 0.20 and 0.40) were also synthesised, however these materials were not employed in catalytic studies due to poor particle morphology and high pyrophoricity.

The aluminium content in the sMAOF(*x*,**A**) samples was determined by ICP-MS analysis, which shows a progressive decrease in Al with increasing **A** loading from 39.5 wt% for the control sMAO to 16.1 wt% in the sMAOF(0.40,**A**). This is consistent with the replacement of Al bound methyl groups with heavier linker modifier groups. The amount of fluorine, as quantified by elemental analysis shows a steady increase with modifier loading from 0.99 wt% for sMAOF(0.001,**A**) and 22.4 wt% for sMAOF(0.40,**A**), consistent with an increase in –O(C_6F_4)O– linker concentration.

Linker modified sMAOF samples were sealed under argon in glass capillaries and X-ray total scattering data were collected at the Diamond Light Source XPDF beamline, I15-1. These data were processed using GudrunX[107,108] with an argon-filled capillary used for the subtraction of the background contributions. The resulting X-ray PDFs are presented in Fig. 3 and S15–S17† and we use the normalisation $D(r)$, as defined by Keen.[102] There are systematic changes in $D(r)$ with increased modifier loading – most clearly in peaks at 1.34, 2.36, 2.84 and 3.62 Å – and peaks are also observed in these positions in the PDF of pure HO(C_6F_4)OH. This provides further evidence for incorporation of –O(C_6F_4)O– units in the sMAOF, which have a rigid structure and, therefore a significant effect on the PDF.

The first and most intense peak for the sMAO sample at *ca.* 1.8 Å arises from Al–O and Al–C correlations, which make up the aluminoxane backbone. This peak decreases in intensity with increased modifier loading, and the peak maximum shows a slight, but progressive, decrease in r from 1.82 Å in sMAO to 1.78 Å in sMAOF(0.40,**A**). These observations can be attributed to the reduced number of Al–C bonds as "structural" TMA reacts to forms Al–O bonds in the modified material. Similar trends are seen in peaks at 3.1 Å and 4.5 Å; which represent Al–Al, Al–O and C–O correlations in unmodified sMAO, and their decreasing intensity is consistent with diminishing number of Al–O–Al moieties as the modifier breaks up the aluminoxane clusters. There is further evidence of aluminoxane clusters being broken up as features in $D(r)$ at

Table 1 Characterisation data for sMAOF(**A**) modified activating supports with different 1,4-HO(C_6F_4)OH modifier loadings

Modifier loading ($[M]_0/[Al_{sMAO}]_0$)	BET[a] ($m^2\ g^{-1}$)	Micropore area[b] ($m^2\ g^{-1}$)	Micropore volume[b] ($cm^3\ g^{-1}$)	Al wt%	F wt%
0	688.9	227.1	0.0952	39.5	0
0.01	750.6	359.0	0.141	37.0	0.99
0.025	785.6	456.4	0.181	31.5	2.47
0.05	895.7	529.1	0.214	29.3	4.44

[a] Specific surface area determined using the BET method.[99] [b] Micropore area and volume determined using *t*-plot analysis.[101] External area = BET surface area – micropore area.

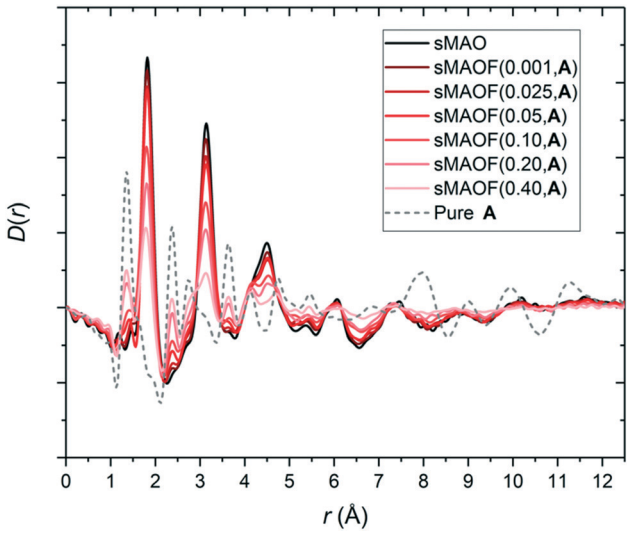

Fig. 3 Overlaid X-ray PDFs of sMAOF(A) with variable loadings of $HO(C_6F_4)OH$.

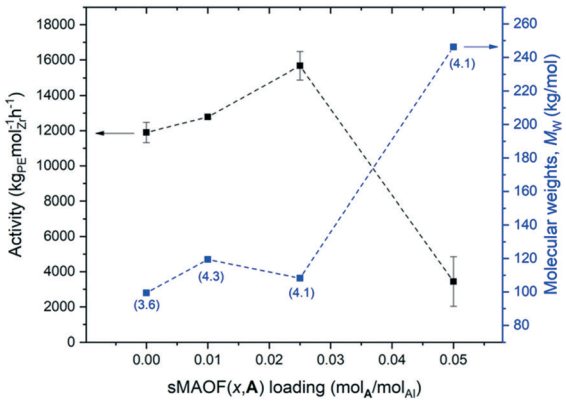

Fig. 4 Ethylene polymerisation activities for $(EBI)ZrCl_2$ supported on sMAOF(A) with variable loadings of $HO(C_6F_4)OH$. Activity (kg_{PE} mol_{Zr}^{-1} h^{-1}) in black; molecular weights, M_w (g mol^{-1}), in blue; and polydispersities, M_w/M_n, in parentheses.

higher-*r* become less defined with greater modifier loading. Scanning electron microscopy (SEM) with energy sispersive X-ray (EDX) spectroscopy of sMAOF(0.40,**A**) confirms a homogeneous distribution of aluminium and fluorine on the surface of the particles (Fig. S18†).

Slurry phase ethylene polymerisation studies with tetrafluorohydroquinone-modified sMAOF supports

Zirconocene complex $(EBI)ZrCl_2$ was selected as a control precatalyst, given its robust structure, high activity for the slurry-phase polymerisation reactions and straightforward comparison with literature studies.[63,109–113] Complete immobilisation of $(EBI)ZrCl_2$ on sMAOF(*x*,**A**) samples with x = 0.01, 0.025, 0.05, was achieved by addition of toluene to a mixture of solid support and complex ($[Al_{sMAOF}]_0/[Zr]_0$ = 200), affording an orange coloured solid below a colourless supernatant solution. The coloured solids were isolated by decantation and dried *in vacuo* and all catalysts were tested for slurry phase ethylene polymerisation capability. The received polymers were free-flowing powders and show no evidence of reactor fouling.

Full polymerisation data are listed in Table S5† and a graphical summary is shown in Fig. 4. The optimum polymerisation activity is found at $[M]_0/[Al_{sMAO}]_0$ = 0.025, with an observed activity of 15.7×10^3 kg_{PE} mol_{Zr}^{-1} h^{-1}, so this modifier loading was used in subsequent solid supports with a range of other aromatic diol linkers (*vide infra*).

The GPC data for the polyethylene produced by $(EBI)ZrCl_2$–sMAOF(*x*,**A**) catalyst systems show larger molecular weights ($108 < M_w < 246$ kDa) *versus* the control (M_w = 99.4 kDa), with a general increase in M_w with increasing linker loading, with the exception of $(EBI)ZrCl_2$–sMAOF(0.025,**A**) as a slight outlier (M_w = 119 kDa). Molecular weight distributions (M_w/M_n) are slightly broader for $(EBI)ZrCl_2$–sMAOF(*x*,**A**) catalysts (4.1–4.3) than for the control (M_w/M_n = 3.6), suggesting slightly greater active site heterogeneity in the linker modified systems.

Polymer morphology is known to be influenced by the catalyst support, which acts as a template for the growing polymer chain in heterogeneous polymerisation.[114–118] Scanning electron microscopy (SEM) images of polyethylene samples for $[M]_0/[Al_{sMAO}]_0$ = 0, 0.01 and 0.025 (Fig. 5a–c, respectively) show retention and replication of the 'popcorn' morphology of the original supports during catalyst immobilisation and polymerisation.[70,71] Replication of the support morphology for the polymers indicates that the supported catalyst has a uniform distribution of active sites and high porosity.

However, in the case of the $[M]_0/[Al_{sMAO}]_0$ = 0.05 supports, a 'bobble-like' texture is observed on the PE particle surface (Fig. 5d and 6). This abnormal surface structure is consistent with the low polymerisation activity observed for the $(EBI)ZrCl_2$–sMAOF(0.05,**A**) catalyst system compared with the control (3.4×10^3 *vs.* 11.9×10^3 kg_{PE} mol_{Zr}^{-1} h^{-1} respectively).

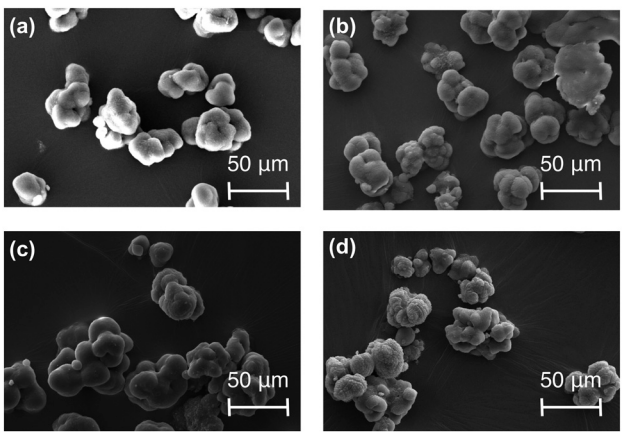

Fig. 5 SEM images (×500 magnification) of PE samples from catalysts based on (a) unmodified and (b)–(d) sMAOF(**A**) for $[M]_0/[Al_{sMAO}]_0$ = 0.01, 0.025 and 0.05.

This may be explained by the lower concentration of $[AlMe_2]^+$ species at higher linker loading, which are often cited as the main responsible species for zirconocene activation.[65] It is also possible that the very high BET surface area observed for the sMAOF(0.05,**A**) support (29.1 m^2 $mmol^{-1}$) results in a non-uniform distribution of active sites during complex immobilisation.

Taking sMAOF(0.025,**A**) as the most activating support for (EBI)$ZrCl_2$ we investigated the effect of increasing [Zr] loading on higher surface area modified support. (EBI)$ZrCl_2$ was immobilised on sMAOF(0.025,**A**) at $[Al_{sMAOF}]_0/[Zr]_0$ = 50, 100, 150, 200 by swirling a toluene slurry of complex and support at 60 °C. In each case complex was fully immobilised as judged by a colourless supernatant solution. Slurry phase ethylene polymerisation data are summarised in Fig. 7, showing catalyst activity increases with increasing $[Al_{sMAOF}]_0/[Zr]_0$ ratio. This is consistent with our previous observations for {(η^5-C_9Me_6)Me_2Si(η^5-C_5H_4)}$ZrCl_2$ supported on sMAO and C_6F_5OH modified-sMAO,[77] and could suggest that at a higher catalyst loading, a lower proportion of the individual Zr sites are activated. However, we cannot rule out the occurrence of mass transport limitations under the conditions employed.

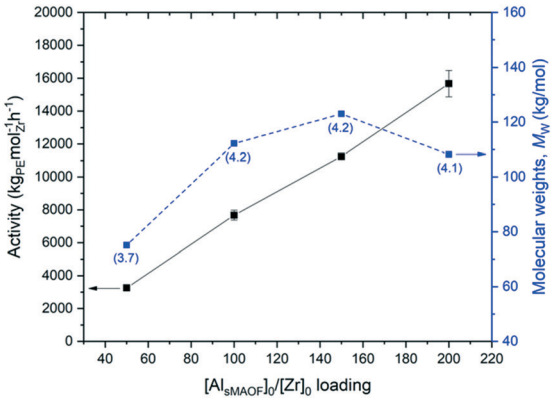

Fig. 7 Ethylene polymerisation activities for (EBI)$ZrCl_2$ supported on sMAOF(0.025,**A**) with variable $[Al_{sMAOF}]_0/[Zr]_0$ loadings. Activity (kg_{PE} mol_{Zr}^{-1} h^{-1}) in black; molecular weights, M_w (g mol^{-1}), in blue; and polydispersities, M_w/M_n, in parentheses.

Synthesis and characterisation of sMAOF materials with aromatic diols

To investigate the scope of these novel sMAOF supports a study into the effect of various aromatic di-ol compounds as sMAO modifiers was carried out. The selection of target linker groups was selected on the basis of price, commercial availability and simple trends in chemical structure.

Due to the significantly lower price of aryl C–H compounds compared with C–F compounds the benzene di-ol compounds hydroquinone 1,4-$(OH)_2C_6H_4$, and resorcinol 1,3-$(OH)_2C_6H_4$ (**C** and **D** in Chart 4) were selected. These allow a simple comparison with the tetrafluorohydroquinone derivative **A**, to see if the same boost in ethylene polymerisation activity can be delivered more economically. To investigate the effect of spacer length, three diphenol derivatives were selected: 4,4′-biphenol (HO)C_6H_4–C_6H_4(OH), $(CH_3)_2C(C_6H_4OH)_2$, and $(CF_3)_2C(C_6H_4$-$OH)_2$ (**E**–**G** in Chart 4). The bisphenol A derivatives **F** and **G** were selected to study the effect of CH_3 *vs.* CF_3 groups on the linker modified sMAOF support. Finally, the effect of different aromatic linker was investigated, using two isomers of naphthalene-diol, 2,5-$(OH)_2(C_{10}H_6)$ and 2,6-$(OH)_2(C_{10}H_6)$ (**H** and **I** in Chart 4).

Upon addition of these aromatic di-ol modifiers to sMAO, effervescence was observed in all cases, confirming a protonolysis reaction with concomitant release of methane gas. All synthesised sMAOF(0.0025,M) samples were characterised by ICP-MS and N_2 physisorption studies (Table 2).

The BET surface area of sMAOF(0.025,M) samples with linker modifiers **C**–**I** (range = 405.0–664.2 m^2 g^{-1}), are all lower that of the control (688.9 m^2 g^{-1}). This suggests that the proposed cross-linker effect, increasing the surface are of the sMAOF, is unique to linker modifier **A**.

X-ray total scattering data for sMAOF(**C**) and sMAOF(**E**) samples (Fig. S16 and S17,† respectively), are consistent with incorporation of the –O(Ar)O– linker groups in the modified solids. It is postulated that the structural modification in these cases has a destabilising effect on the sMAOF clusters.

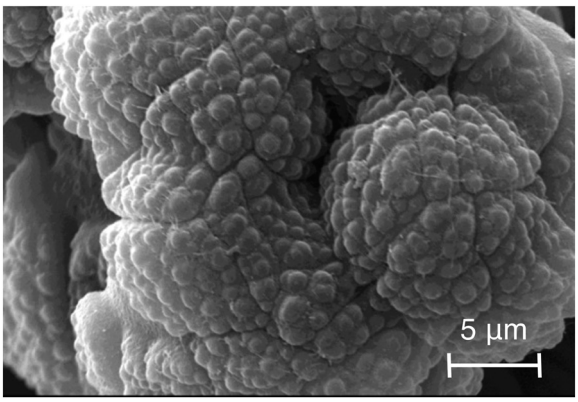

Fig. 6 SEM image (×4000 magnification) of PE samples from a catalyst based on sMMAO(0.05,**A**).

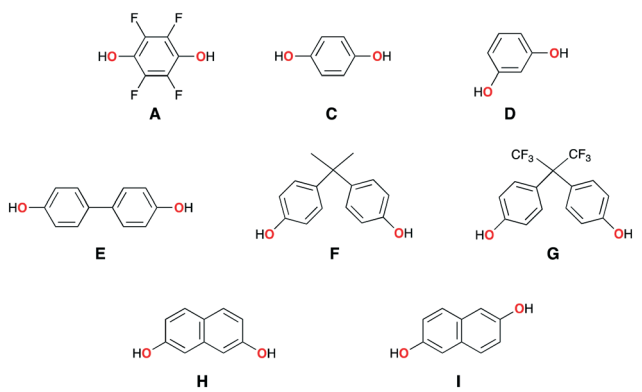

Chart 4 Diol linker modifiers selected for this study.

Table 2 Characterisation data for solid MAO supports modified at 2.5 mol% initial loading and slurry phase ethylene polymerisation data with (EBI)$ZrCl_2$ supported precatalysts

Modifier	BET (m^2 g^{-1})	Al wt%	Activity/10^3 (kg_{PE} mol_{Zr}^{-1} h^{-1})	M_w (kDa)	M_w/M_n
Control	688.9	39.0	11.9	99.4	3.6
A	785.6	31.5	15.7	119	4.3
C	664.2	32.7	11.3	129	4.2
D	656.1	32.0	13.2	152	4.2
E	656.1	23.7	12.8	129	4.3
F	656.7	33.6	9.04	135	3.9
G	580.5	26.0	4.98	192	4.0
H	405.0	33.6	10.7	133	4.2
I	631.8	28.2	12.7	119	4.0

Polymerisation conditions: 10 mg catalyst, 2 bar C_2H_4, 70 °C, 30 minutes, $[Al_{TIBA}]_0/[Zr]_0$ = 1000, hexanes (50 mL). All polymerisation experiments were conducted at least twice to ensure the reproducibility of the corresponding outcome and mean activity values are quoted correct to 3 significant figures.

Table 3 Characterisation and scale-up ethylene polymerisation data for solid MAO supports modified at $[M]_0/[Al_{sMAO}]_0$ = 0.025, and slurry phase ethylene polymerisation data with (EBI)$ZrCl_2$ supported precatalysts

Modifier	Support Al wt%	Catalyst [Al]/[Zr]	Activity/10^3 (kg_{PE} mol_{Zr}^{-1} h^{-1})	M_w (kDa)	M_w/M_n
Control	35.2	199	116	99.9	3.6
C_6F_5OH	31.6	226	140	87.3	3.9
A	31.5	179	163	122	4.3
C	32.7	178	99.5	129	4.3
D	35.2	178	81.7	155	4.2
E	33.7	178	103	134	4.0
I	28.2	195	108	118	4.0

Polymerisation conditions: 25.0 mg catalyst, 8 bar C_2H_4, 80 °C, 60 minutes, 2.5 mL triethylaluminium, 1000 mL hexanes. All polymerisation experiments were conducted at least twice to ensure the reproducibility of the corresponding outcome and mean activity values are quoted correct to 3 significant figures.

Slurry phase ethylene polymerisation studies

The complex (EBI)$ZrCl_2$ was immobilised on the surface of the linker modified sMAOF(0.025,M) samples and all catalysts were tested for polymerisation capability in a 150 mL ampoule reactor at an ethylene pressure of 2 bar. The average activity data for each polymerisation reaction are collated in Table 2. The polymerisation activity is slightly boosted in the case of M = **D**, **E** and **I** (13.2, 12.8, and 12.7 × 10^3 kg_{PE} mol_{Zr}^{-1} h^{-1}, respectively) with respect to the control catalyst system (11.9 × 10^3 kg_{PE} mol_{Zr}^{-1} h^{-1}). These data suggest that an electron withdrawing aryl-fluoride modifier is not a strict requirement for a highly active catalyst support. The remaining linker modifiers M = **C**, **F**, **G**, **H** show lower activity values with respect to the control catalyst (11.3, 9.04, 4.98, and 10.7 × 10^3 kg_{PE} mol_{Zr}^{-1} h^{-1}, respectively), and no clear structure/activity trends between the structure of the linker or the surface area of the sMAOF are apparent.

Scale-up polymerisation studies carried in a 2 L reactor at an ethylene pressure of 8 bar (Table 3, Fig. S23†) confirm sMAOF(0.025,**A**) as the most activating support for the (EBI)$ZrCl_2$ immobilised catalyst showing a value of 163 × 10^3 kg_{PE} mol_{Zr}^{-1} h^{-1}, which corresponds to a +40% and +17% increase with respect to the control and C_6F_5OH-modified sMAO supports, respectively (116 × 10^3 and 140 × 10^3 kg_{PE} mol_{Zr}^{-1} h^{-1}, respectively). The GPC data for the polyethylene produced by (EBI)$ZrCl_2$ supported on sMAOF(0.025,M) show molecular weight (M_w) values, ranging from 155 to 118 kg mol^{-1} (Fig. S27†). These are higher M_w values than those for the control catalyst (99.4 kg mol^{-1}) and an analogous catalyst system based on C_6F_5OH modified sMAO (87.3 kg mol^{-1}). A decrease in M_w can be attributed to an enhancement of chain transfer to aluminium,[119,120] which is promoted by an increased concentration of Lewis acid sites, and a decrease in surface area in the C_6F_5OH modified sMAO catalyst systems.[76] This problem is circumvented in the sMAOF based catalysts, which can be correlated with the larger surface areas with these modified supports. Higher polymer M_w values could also be explained by a decrease in "free" TMA in the diol-modified catalyst systems with respect to unmodified sMAO.[24,26,29,121–125]

Conclusions

Samples of solid polymethylaluminoxane have been modified with 8 different aryl di-ol modifier reagents on a gram scale. These solids have been extensively characterised using ICP-MS analysis, diffuse-reflectance FT-IR, solution and solid state NMR spectroscopy, SEM–EDX, X-ray PDF and N_2 physisorption studies.

DRIFT spectroscopy confirms that no hydroxy groups are present in the modified samples, consistent with a double deprotonation of the aryl diol O–H groups, producing

methane (CH_4) and two new Al–O bonds. Solution and solid state ^{19}F NMR spectra with linker modifier **A** are consistent with the incorporation of a $–O(C_6F_4)O–$ group between sMAO sub-units in a cross-linked structure, described as a solid polymethylaluminoxane organic framework (sMAOF). We tentatively propose two "structural" TMA molecules are replaced with one analogous $Me_2Al–O(C_6F_4)O–AlMe_2$. The "structural" groups formed are not labile, and bind strongly to type I and/or type II Lewis acid sites in the MAO cluster, with one $–O(C_6F_4)O–$ ligand bridging two Al centres at each end, on two separate cluster sites.

^1H NMR spectroscopy data in THF-d_8 reveal that sMAOF(**A**) modified at 2.5 mol% initial loading can generate both $AlMe_3(THF)$ and $[AlMe_2(THF)_2]^+$ species, but at 5 mol% modifier loading results in a significant decrease in ionisation.

ICP-MS, SEM–EDX and X-ray PDF analysis of sMAOF(**A**) confirms the incorporation of $–O(C_6F_4)O–$ units in the solid samples, and an increased modifier loading leads to an increase in linker concentration. N_2 physisorption isotherms reveal that the $HO(C_6F_4)OH$ linker modifier yields a sMAOF with a significantly increased BET surface area and micropore volume with respect to the parent sMAO support.

These novel sMAOF materials were tested as activating supports for a $(EBI)ZrCl_2$ precatalyst in slurry phase ethylene polymerisation studies. At an optimised modifier loading of 2.5 mol%, the polymerisation activity of the $(EBI)ZrCl_2$–sMAOF(**A**) system is increased by +32% (150 mL scale) and +40% (2 L scale) with respect to the $(EBI)ZrCl_2$–sMAO control catalyst, under identical zirconium loading and polymerisation conditions. However, an analogous catalyst system based sMAOF(0.05,**A**) resulted in a significant drop in activity and unusual polymer morphology, which may be explained by a smaller amounts of transient $[AlMe_2]^+$ species being generated at higher linker modifier loadings.

Furthermore, equivalent catalysts supported on alternative diol linkers sMAOF(**C–I**) with $[M]_0/[Al_{sMAO}]_0$ = 0.025, did not provide such a significant boost in polymerisation activity, indicating that a structure/activity relationship in these catalyst systems is more complex than simple trends in surface area of the sMAOF. More research is required into the nature of the active catalytic sites and the possible interaction of the linker modifier, in order to further optimise single-site catalyst performance with sMAOF activating supports.

Conflicts of interest

There are no conflicts to declare.

Acknowledgements

A. F. R. K., Z. R. T. and J.-C. B. thank SCG Chemicals Co., Ltd (Thailand) for funding. H. S. G. acknowledges financial support from the EPSRC. We are grateful to Dr J. V. Lamb (University of Oxford) for SEM imaging, Dr P. Kenyon (University of Oxford) for DRIFTS measurements, Dr N. H. Rees (University of Oxford) for SSNMR spectroscopy and Mrs J. A. Holter (David Cockayne Centre for Electron Microscopy, Oxford Materials) for SEM–EDX analysis. Thanks to Dr C. Chen (University of Oxford) and C. Pilkington (Micromeritics Ltd) for assistance with the N_2 physisorption studies. We acknowledge the Diamond Light Source, U.K. for the allocation of beamtime (sessions EE16072 and EE19128) and thank Dr D. Keeble and all the staff of Beamline I15-1 for assistance with the XPDF measurements. We thank Dr S. Sripothongnak, Dr N. Nealmongkolrattana and Mr T. Parawan (SCG Chemicals Co., Ltd) for assistance with modification reactions and scale up polymerisation testing. A. F. R. K. also thanks Wadham College Oxford for a R. J. P. Williams Junior Research Fellowship.

Notes and references

1 A. Andresen, H.-G. Cordes, J. Herwig, W. Kaminsky, A. Merck, R. Mottweiler, J. Pein, H. Sinn and H.-J. Vollmer, *Angew. Chem., Int. Ed. Engl.*, 1976, **15**, 630–632.
2 W. Kaminsky, *Organometallics*, 2012, **45**, 3289–3297.
3 H. S. Zijlstra and S. Harder, *Eur. J. Inorg. Chem.*, 2014, **2015**, 19–43.
4 F. Ghiotto, C. Pateraki, J. Tanskanen, J. R. Severn, N. Luehmann, A. Kusmin, J. Stellbrink, M. Linnolahti and M. Bochmann, *Organometallics*, 2013, **32**, 3354–3362.
5 M. A. Henderson, T. K. Trefz, S. Collins, M. Y. Wang and J. S. McIndoe, *Organometallics*, 2013, **32**, 2079–2083.
6 T. K. Trefz, M. A. Henderson, M. Y. Wang, S. Collins and J. S. McIndoe, *Organometallics*, 2013, **32**, 3149–3152.
7 T. K. Trefz, M. A. Henderson, M. Linnolahti, S. Collins and J. S. McIndoe, *Chem. – Eur. J.*, 2015, **21**, 2980–2991.
8 H. S. Zijlstra, M. C. A. Stuart and S. Harder, *Organometallics*, 2015, **48**, 5116–5119.
9 N. Tymińska and E. Zurek, *ACS Catal.*, 2015, **5**, 6989–6998.
10 H. S. Zijlstra, M. Linnolahti, S. Collins and J. S. McIndoe, *Organometallics*, 2017, **36**, 1803–1809.
11 S. Collins, M. Linnolahti, M. G. Zamora, H. S. Zijlstra, M. T. Rodríguez Hernández and O. Perez-Camacho, *Macromolecules*, 2017, **50**, 8871–8884.
12 H. Zijlstra, S. Collins and J. S. McIndoe, *Chem. – Eur. J.*, 2018, **24**, 5506–5512.
13 H. S. Zijlstra, A. Joshi, M. Linnolahti, S. Collins and J. S. McIndoe, *Dalton Trans.*, 2018, **47**, 17291–17298.
14 H. S. Zijlstra, A. Joshi, M. Linnolahti, S. Collins and J. S. McIndoe, *Eur. J. Inorg. Chem.*, 2019, **2019**, 2346–2355.
15 A. Joshi, H. S. Zijlstra, E. Liles, C. Concepcion, M. Linnolahti and J. S. McIndoe, *Chem. Sci.*, 2021, **12**, 546–551.
16 A. Joshi, S. Collins, M. Linnolahti, H. S. Zijlstra, E. Liles and J. S. McIndoe, *Chem. – Eur. J.*, 2021, **27**, 8753–8763.
17 K. R. Robert and D. D. VanderLende, *US Pat.*, 5919983A, 1999.
18 H. J. Lee, J. W. Baek, Y.-H. Seo, H.-C. Lee, S. M. Jeong, J. Lee, C.-G. Lee and B. Y. Lee, *Molecules*, 2021, **26**, 2827.
19 I. M. Riddlestone, A. Kraft, J. Schaefer and I. Krossing, *Angew. Chem., Int. Ed.*, 2018, **57**, 13982–14024.

20 S. O. Gunther, Q. Lai, T. Senecal, R. Huacuja, S. Bremer, D. M. Pearson, J. C. DeMott, N. Bhuvanesh, O. V. Ozerov and J. Klosin, *ACS Catal.*, 2021, **11**, 3335–3342.
21 F. Zaccaria, C. Zuccaccia, R. Cipullo, P. H. M. Budzelaar, A. Vittoria, A. Macchioni, V. Busico and C. Ehm, *ACS Catal.*, 2021, 4464–4475.
22 T. Nakashima, Y. Nakayama, T. Shiono and R. Tanaka, *ACS Catal.*, 2021, **11**, 865–870.
23 M. D. Healy, D. A. Wierda and A. R. Barron, *Organometallics*, 1988, **7**, 2543–2548.
24 V. Busico, R. Cipullo, F. Cutillo, N. Friederichs, S. Ronca and B. Wang, *J. Am. Chem. Soc.*, 2003, **125**, 12402–12403.
25 A. Tynys, J. L. Eilertsen, J. V. Seppälä and E. Rytter, *J. Polym. Sci., Part A: Polym. Chem.*, 2007, **45**, 1364–1376.
26 F. Ghiotto, C. Pateraki, J. R. Severn, N. Friederichs and M. Bochmann, *Dalton Trans.*, 2013, **42**, 9040–9048.
27 L. Rocchigiani, V. Busico, A. Pastore and A. Macchioni, *Dalton Trans.*, 2013, **42**, 9104–9111.
28 F. Zaccaria, P. H. M. Budzelaar, R. Cipullo, C. Zuccaccia, A. Macchioni, V. Busico and C. Ehm, *Inorg. Chem.*, 2020, **59**, 5751–5759.
29 F. Zaccaria, C. Zuccaccia, R. Cipullo, P. H. M. Budzelaar, A. Macchioni, V. Busico and C. Ehm, *ACS Catal.*, 2019, **9**, 2996–3010.
30 F. Zaccaria, C. Zuccaccia, R. Cipullo, P. H. M. Budzelaar, A. Macchioni, V. Busico and C. Ehm, *Eur. J. Inorg. Chem.*, 2020, **2020**, 1088–1095.
31 S. Ronca, D. Romano, G. Forte, E. Andablo-Reyes and S. Rastogi, *Adv. Polym. Technol.*, 2012, **31**, 193–204.
32 S. Mark, A. Kurek, R. Mülhaupt, R. Xu, G. Klatt, H. Köppel and M. Enders, *Angew. Chem., Int. Ed.*, 2010, **49**, 8751–8754.
33 F. Rouholahnejad, D. Mathis and P. Chen, *Organometallics*, 2010, **29**, 294–302.
34 A. Tynys, J. L. Eilertsen and E. Rytter, *Macromol. Chem. Phys.*, 2006, **207**, 295–303.
35 E. Zurek, T. K. Woo, A. T. K. Firman and T. Ziegler, *Inorg. Chem.*, 2001, **40**, 361–370.
36 E. Zurek and T. Ziegler, *Inorg. Chem.*, 2001, **40**, 3279–3292.
37 E. Zurek and T. Ziegler, *Prog. Polym. Sci.*, 2004, **29**, 107–148.
38 M. Linnolahti, J. R. Severn and T. A. Pakkanen, *Angew. Chem., Int. Ed.*, 2006, **45**, 3331–3334.
39 L. Negureanu, R. W. Hall, L. G. Butler and L. A. Simeral, *J. Am. Chem. Soc.*, 2006, **128**, 16816–16826.
40 M. Linnolahti, J. R. Severn and T. A. Pakkanen, *Angew. Chem., Int. Ed.*, 2008, **47**, 9279–9283.
41 R. Glaser and X. Sun, *J. Am. Chem. Soc.*, 2011, **133**, 13323–13336.
42 Z. Boudene, T. de Bruin, H. Toulhoat and P. Raybaud, *Organometallics*, 2012, **31**, 8312–8322.
43 Z. Falls, N. Tymińska and E. Zurek, *Macromolecules*, 2014, **47**, 8556–8569.
44 Z. Falls, E. Zurek and J. Autschbach, *Phys. Chem. Chem. Phys.*, 2016, **18**, 24106–24118.
45 M. Linnolahti, A. Laine and T. A. Pakkanen, *Chem. – Eur. J.*, 2013, **19**, 7133–7142.
46 J. T. Hirvi, M. Bochmann, J. R. Severn and M. Linnolahti, *ChemPhysChem*, 2014, **15**, 2732–2742.
47 M. Linnolahti and S. Collins, *ChemPhysChem*, 2017, **18**, 3369–3374.
48 S. Collins, G. Hasan, A. Joshi, J. S. McIndoe and M. Linnolahti, *ChemPhysChem*, 2021, **22**, 1326–1335.
49 *Tailor-Made Polymers*, ed. J. R. Severn and J. C. Chadwick, Wiley-VCH Verlag GmbH & Co. KGaA, Weinheim, Germany, 2008.
50 J. R. Severn, J. C. Chadwick, R. Duchateau and N. Friederichs, *Chem. Rev.*, 2005, **105**, 4073–4147.
51 C. Janiak, B. Rieger, R. Voelkel and H.-G. Braun, *J. Polym. Sci., Part A: Polym. Chem.*, 1993, **31**, 2959–2968.
52 J. Jin, T. Uozumi and K. Soga, *Macromol. Chem. Phys.*, 1996, **197**, 849–854.
53 J. Wang, J. Chen and Y. Yang, *J. Supercrit. Fluids*, 2005, **33**, 159–172.
54 M. Bartke, M. Oksman, M. Mustonen and P. Denifl, *Macromol. Mater. Eng.*, 2005, **290**, 250–255.
55 J. C. Hicks, B. A. Mullis and C. W. Jones, *J. Am. Chem. Soc.*, 2007, **129**, 8426–8427.
56 M. O. Kristen, *Top. Catal.*, 1999, **7**, 89–95.
57 G. G. Hlatky, *Chem. Rev.*, 2000, **100**, 1347–1376.
58 M. C. Baier, M. A. Zuideveld and S. Mecking, *Angew. Chem., Int. Ed.*, 2014, **53**, 9722–9744.
59 M. M. Stalzer, M. Delferro and T. J. Marks, *Catal. Lett.*, 2015, **145**, 3–14.
60 S. S. Reddy and S. Sivaram, *Prog. Polym. Sci.*, 1995, **20**, 309–367.
61 L. Resconi, L. Cavallo, A. Fait and F. Piemontesi, *Chem. Rev.*, 2000, **100**, 1253–1346.
62 J.-N. Pédeutour, K. Radhakrishnan, H. Cramail and A. Deffieux, *Macromol. Rapid Commun.*, 2001, **22**, 1095–1123.
63 M. C. Haag, C. Krug, J. Dupont, G. B. de Galland, J. H. Z. dos Santos, T. Uozumi, T. Sano and K. Soga, *J. Mol. Catal. A: Chem.*, 2001, **169**, 275–287.
64 D. Bianchini, J. H. Z. dos Santos, T. Uozumi and T. Sano, *J. Mol. Catal. A: Chem.*, 2002, **185**, 223–235.
65 M. E. Z. Velthoen, H. Meeldijk, F. Meirer and B. M. Weckhuysen, *Chem. – Eur. J.*, 2018, **24**, 11944–11953.
66 V. N. Panchenko, N. V. Semikolenova, I. G. Danilova, E. A. Paukshtis and V. A. Zakharov, *J. Mol. Catal. A: Chem.*, 1999, **142**, 27–37.
67 M. A. Bashir, T. Vancompernolle, R. M. Gauvin, L. Delevoye, N. Merle, V. Monteil, M. Taoufik, T. F. L. McKenna and C. Boisson, *Catal. Sci. Technol.*, 2016, **6**, 2962–2974.
68 M. E. Z. Velthoen, A. Muñoz-Murillo, A. Bouhmadi, M. Cecius, S. Diefenbach and B. M. Weckhuysen, *Organometallics*, 2018, **51**, 343–355.
69 E. Kaji and E. Yoshioka, *US Pat.*, US8404880B2, 2013.
70 A. F. R. Kilpatrick, J.-C. Buffet, P. Nørby, N. H. Rees, N. P. Funnell, S. Sripothongnak and D. O'Hare, *Chem. Mater.*, 2016, **28**, 7444–7450.
71 J.-C. Buffet, Z. Turner and D. O'Hare, *Chem. Commun.*, 2018, **54**, 10970–10973.

72 J. Lamb, J.-C. Buffet, Z. Turner and D. O'Hare, *Polym. Chem.*, 2019, **10**, 1386–1398.
73 P. Angpanitcharoen, J. V. Lamb, J.-C. Buffet, Z. R. Turner and D. O'Hare, *RSC Adv.*, 2021, **11**, 11529–11535.
74 T. A. Q. Arnold, Z. R. Turner, J.-C. Buffet and D. O'Hare, *J. Organomet. Chem.*, 2016, **822**, 85–90.
75 J.-C. Buffet, T. A. Q. Arnold, Z. R. Turner, P. Angpanitcharoen and D. O'Hare, *RSC Adv.*, 2015, **5**, 87456–87464.
76 A. F. R. Kilpatrick, N. H. Rees, S. Sripothongnak, J.-C. Buffet and D. O'Hare, *Organometallics*, 2018, **37**, 156–164.
77 J. V. Lamb, J.-C. Buffet, Z. R. Turner and D. O'Hare, *Macromolecules*, 2020, **53**, 929–935.
78 A. F. R. Kilpatrick, N. H. Rees, Z. R. Turner, J.-C. Buffet and D. O'Hare, *Mater. Chem. Front.*, 2020, **4**, 3226–3233.
79 N. Popoff, J. Espinas, J. Pelletier, K. C. Szeto, J. Thivolle-Cazat, L. Delevoye, R. M. Gauvin and M. Taoufik, *ChemCatChem*, 2013, **5**, 1971–1977.
80 N. Popoff, K. C. Szeto, N. Merle, J. Espinas, J. Pelletier, F. Lefebvre, J. Thivolle-Cazat, L. Delevoye, A. De Mallmann, R. M. Gauvin and M. Taoufik, *Catal. Today*, 2014, **235**, 41–48.
81 N. Popoff, B. Macqueron, W. Sayhoun, J. Espinas, J. Pelletier, O. Boyron, C. Boisson, N. Merle, K. C. Szeto, R. M. Gauvin, A. De Mallmann and M. Taoufik, *Eur. J. Inorg. Chem.*, 2014, **2014**, 888–895.
82 M. Kioka and N. Kashiwa, *US Pat.*, US4952540, 1990.
83 D. Fischer, S. Jüngling and R. Mülhaupt, *Macromol. Symp.*, 1993, **66**, 191–202.
84 L. C. T. Shoute, J. P. Mittal and P. Neta, *J. Phys. Chem.*, 1996, **100**, 3016–3019.
85 T. Mole, *Aust. J. Chem.*, 1966, **19**, 373–379.
86 M. Skowrońska-Ptasińska, K. B. Starowieyski, S. Pasynkiewicz and M. Carewska, *J. Organomet. Chem.*, 1978, **160**, 403–409.
87 V. Belot, D. Farran, M. Jean, M. Albalat, N. Vanthuyne and C. Roussel, *J. Org. Chem.*, 2017, **82**, 10188–10200.
88 S. A. Cantalupo, H. E. Ferreira, E. Bataineh, A. J. King, M. V. Petersen, T. Wojtasiewicz, A. G. DiPasquale, A. L. Rheingold and L. H. Doerrer, *Inorg. Chem.*, 2011, **50**, 6584–6596.
89 K. Ishihara, N. Hanaki and H. Yamamoto, *J. Am. Chem. Soc.*, 1991, **113**, 7074–7075.
90 K. Ishihara, N. Hanaki and H. Yamamoto, *J. Am. Chem. Soc.*, 1993, **115**, 10695–10704.
91 D. S. McGuinness, A. J. Rucklidge, A. R. P. Tooze and A. M. Z. Slawin, *Organometallics*, 2007, **26**, 2561–2569.
92 E. Y. Chen and T. J. Marks, *Chem. Rev.*, 2000, **100**, 1391–1434.
93 F. Zaccaria, L. Sian, C. Zuccaccia and A. Macchioni, *Adv. Organomet. Chem.*, 2020, **73**, 1–78.
94 J. L. Eilertsen, J. A. Støvneng, M. Ystenes and E. Rytter, *Inorg. Chem.*, 2005, **44**, 4843–4851.
95 A. Laine, M. Linnolahti and T. A. Pakkanen, *J. Organomet. Chem.*, 2012, **716**, 79–85.
96 C. Bergquist, B. M. Bridgewater, C. J. Harlan, J. R. Norton, R. A. Friesner and G. Parkin, *J. Am. Chem. Soc.*, 2000, **122**, 10581–10590.
97 A. G. Massey and A. J. Park, *J. Organomet. Chem.*, 1964, **2**, 245–250.
98 P. Hodgkinson, *Prog. Nucl. Magn. Reson. Spectrosc.*, 2005, **46**, 197–222.
99 S. Brunauer, P. H. Emmett and E. Teller, *J. Am. Chem. Soc.*, 1938, **60**, 309–319.
100 M. Thommes, K. Kaneko, A. V. Neimark, J. P. Olivier, F. Rodriguez-Reinoso, J. Rouquerol and K. S. W. Sing, *Pure Appl. Chem.*, 2015, **87**, 1051–1069.
101 B. C. Lippens and J. H. De Boer, *J. Catal.*, 1965, **4**, 319–323.
102 D. A. Keen, *J. Appl. Crystallogr.*, 2001, **34**, 172–177.
103 B. V. K. J. Schmidt, *Macromol. Rapid Commun.*, 2020, **41**, 1900333.
104 T. A. Goetjen, J. Liu, Y. Wu, J. Sui, X. Zhang, J. T. Hupp and O. K. Farha, *Chem. Commun.*, 2020, **56**, 10409–10418.
105 R. C. Klet, S. Tussupbayev, J. Borycz, J. R. Gallagher, M. M. Stalzer, J. T. Miller, L. Gagliardi, J. T. Hupp, T. J. Marks, C. J. Cramer, M. Delferro and O. K. Farha, *J. Am. Chem. Soc.*, 2015, **137**, 15680–15683.
106 P. Ji, J. B. Solomon, Z. Lin, A. M. Wilders, R. F. Jordan and W. Lin, *J. Am. Chem. Soc.*, 2017, **139**, 11325–11328.
107 A. K. Soper and E. R. Barney, *J. Appl. Crystallogr.*, 2011, **44**, 714–726.
108 A. K. Soper, *GudrunN and GudrunX: programs for correcting raw neutron and X-ray diffraction data to differential scattering cross section*, Science & Technology Facilities Council Swindon, UK, 2011.
109 S. Collins, W. M. Kelly and D. A. Holden, *Organometallics*, 1992, **25**, 1780–1785.
110 J. Tudor and D. O'Hare, *Chem. Commun.*, 1997, 603–604.
111 R. Guimarães, F. C. Stedile and J. H. Z. dos Santos, *J. Mol. Catal. A: Chem.*, 2003, **206**, 353–362.
112 J.-C. Buffet, Z. R. Turner, R. T. Cooper and D. O'Hare, *Polym. Chem.*, 2015, **6**, 2493–2503.
113 J.-C. Buffet, N. Wanna, T. A. Q. Arnold, E. K. Gibson, P. P. Wells, Q. Wang, J. Tantirungrotechai and D. O'Hare, *Chem. Mater.*, 2015, **27**, 1495–1501.
114 F. Junges, R. F. de Souza, J. H. Z. dos Santos and O. L. Casagrande, *Macromol. Mater. Eng.*, 2005, **290**, 72–77.
115 R. Xu, D. Liu, S. Wang and B. Mao, *Macromol. Chem. Phys.*, 2006, **207**, 779–786.
116 M. P. Gil and O. L. Casagrande, *Appl. Catal., A*, 2007, **332**, 110–114.
117 H. Jiang, F. He and H. Wang, *J. Polym. Res.*, 2009, **16**, 183–189.
118 E. Kianfar, R. Azimikia and S. M. Faghih, *Catal. Lett.*, 2020, **150**, 2322–2330.
119 E. Quintanilla, F. di Lena and P. Chen, *Chem. Commun.*, 2006, 4309–4311.
120 R. A. Petros and J. R. Norton, *Organometallics*, 2004, **23**, 5105–5107.
121 R. Cipullo, P. Melone, Y. Yu, D. Iannone and V. Busico, *Dalton Trans.*, 2015, **44**, 12304–12311.
122 C. Ehm, R. Cipullo, P. H. M. Budzelaar and V. Busico, *Dalton Trans.*, 2016, **45**, 6847–6855.
123 M. Bochmann and S. J. Lancaster, *Angew. Chem., Int. Ed. Engl.*, 1994, **33**, 1634–1637.

124 D. E. Babushkin, N. V. Semikolenova, V. A. Zakharov and E. P. Talsi, *Macromol. Chem. Phys.*, 2000, **201**, 558–567.

125 C. Ehm, G. Antinucci, P. H. M. Budzelaar and V. Busico, *J. Organomet. Chem.*, 2014, **772–773**, 161–171.